*Structural Engineering and Mechanics, Vol. 9, No. 2 (2000) 111-126*
DOI: http://dx.doi.org/10.12989/sem.2000.9.2.111


# Dynamic nonlinear member failure propagation in truss structures

Ramesh B. Malla†

*Department of Civil & Environmental Engineering, University of Connecticut, Storrs, CT 06269-2037, U.S.A.*

Butchi B. Nalluri‡

*Electro-Motive Division, General Motors Corporation, Lagrange, IL 60525-3267, U.S.A.*

**Abstract.** Truss type structures are attractive to a variety of engineering applications on earth as well as in space due to their high stiffness to mass ratios and ease of construction and fabrication. During the service life, an individual member of a truss structure may lose load carrying capacity due to many reasons, which may lead to collapse of the structure. An analytical and computational procedure has been developed to study the response of truss structures subject to member failure under static and dynamic loadings. Emphasis is given to the dynamic effects of member failure and the propagation of local damage to other parts of the structure. The methodology developed is based on nonlinear finite element analysis technique and considers elasto-plastic material nonlinearity, postbuckling of members, and large deformation geometric nonlinearity. The pseudo force approach is used to represent the member failure. Results obtained for a planar nine-bay indeterminate truss undergoing sequential member failure show that failure of one member can initiate failure of several members in the structure.

**Key words :** truss structures; progressive failure; dynamic member failure; dynamic nonlinear analysis; buckling; post-buckling response; member failure propagation.

## 1. Introduction

Truss type structures are preferred for various large-scale construction projects on land, in ocean, and in space. An individual member or a group of members of the structure may lose load carrying capacity due to the existence of material defects, fabrication errors, overloading, impact, and abnormal loadings. For safety and to account for uncertainties and unpredictabilities in real life environments, these structures are designed to have a large number of redundant members. However, several long-span latticed roofs have collapsed worldwide in the past (ASCE 1984).

Although a member (local) damage affects a small portion of the structure initially, it has potential for propagating to other parts of the structure that may ultimately cause total collapse of the structure (progressive failure). Several studies have been reported on progressive collapse of truss and frame

† Associate Professor
‡ Research Engineer (Previously Graduate Research and Teaching Assistant, Department of Civil & Environmental Engineering, University of Connecticut)

structures under static loading conditions (e.g., Murtha-Smith 1988, Blandford and Wang 1993). However, in reality, the failure or rupture of members during progressive collapse in a lattice truss is realized to be sudden, therefore dynamic in nature (Davies and Neal 1964, Schmidt *et al.* 1976).

Therefore, accurate response of these structures under member failure can only be achieved by considering the actual dynamic nature of the member failure and the inertia forces arising from it. Recently a few studies including in some extent effects of dynamic member failure on the response of the total structure have been reported (Malla *et al.* 1993, 1995, Morris 1993a, b, Malla and Nalluri 1994, 1995). However, a robust nonlinear analysis technique is essential to model the structural response close to the realistic one.

This paper presents an analytical and computational procedure to determine the response of truss structures subject to member failure under static and dynamic loadings. Emphasis is given to the dynamic effects of member failure. The methodology includes the actual member loading and unloading behavior in elastic, elastic buckling, postbuckling, and tension yielding regions and the rate of member capacity reduction (either the sudden or slow reduction of member load carrying capacity). The sequential member failure is studied. The material nonlinearity is modeled in member axial load versus axial deflection space, and the large displacement geometric nonlinearity is included while computing the stiffness of the structure. The analysis consists of determining displacement and member force time-history response. Results are presented for a planar nine-bay truss.

## 2. Methodology

This section presents a brief description of the proposed method to determine the dynamic response of truss structures undergoing nonlinear member failure.

### *2.1. Member behavior models*

Better structural modeling can be achieved if the load-deflection curve for a member is known precisely. The nature of the postbuckling curves dictates the manner in which load in the buckling member is shed to adjacent members. A typical member axial load-axial deformation behavior of a pin-ended member under axial load is as shown in Fig. 1. In the present study, a method similar to Nonaka (1973, 1977) and Papadrakakis (1985) are used for the modeling of member behavior. The relations involved in each stage of deformation that are used in the methodology are presented below (Nalluri 1996).

### *2.2. Member ideal response subjected to cyclic loading*

The behavior of a pin-ended member (Fig. 1) subjected to a cyclic axial load is briefly described in the following sections. The member behavior can be classified into several stages (Chen and Han 1985): (a) elastic compression (OA), (b) elastic buckling (AB), (c) inelastic post buckling (BC), (d) elastic unloading (CD), (e) elastic tensioning (DE), (f) elastic-plastic tensioning (EF), (g) plastic tensioning (FG), and (h) elastic unloading (GH).

The total axial deformation $\Delta$ can be expressed as the sum of four axial displacement components (Nonaka 1973, 1977)

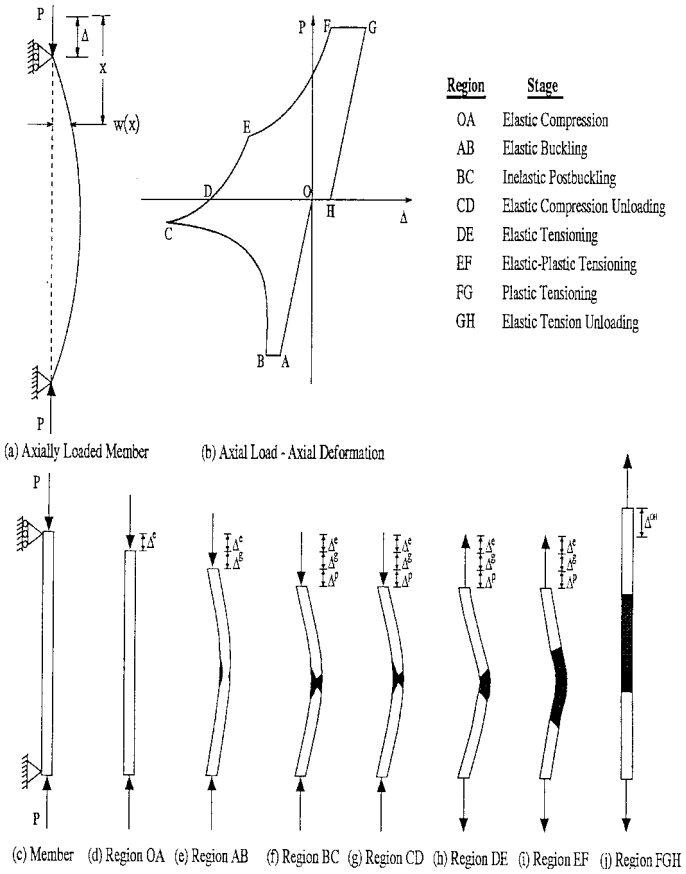


Fig. 1 Typical cyclic axial load-axial displacement relation for a pin-ended member

$$\Delta = \Delta_e + \Delta_g + \Delta_p + \Delta_t \tag{1}$$

where $\Delta_e$ is due to uniform elastic axial deformation; $\Delta_g$ is due to change in geometry associated with lateral deflection ($w$); $\Delta_p$ is due to plastic elongation at the yield hinge; and $\Delta_t$ is due to plastic elongation in tension distributed along the member axis. The axial deformation is considered as positive when the distance between the ends of the bar increases. The axial load ($P$) at the member end is considered as positive for tension load.

A member deforms linearly until the axial load either reaches its Euler buckling load under compression or yield load under tension (Fig. 1d). Only the first right hand term of Eq. (1) contributes to axial deflection during this stage. A small increase in compressive load beyond the Euler's buckling load causes the member to start deflecting in the lateral direction (buckling) without further increase in the load. Due to this lateral deflection, the second term $\Delta_g$ in Eq. (1), comes into picture. The extreme fibers of the cross section at mid length of the pinned ended member start yielding first. The yielding spreads across the cross section and along the member axis depending on the member geometric properties. At point B, a fully plastic hinge forms across the cross section at mid-length of the member when the internal moment equals the plastic moment of the cross section.

Beyond point B, the member exhibits softening behavior, that is, the magnitude of the axial force

$P$ must decrease with increasing magnitude of deflection. At this stage the first three right hand components of Eq. (1) will contribute to the axial deflection. Increase in axial deflection is caused by the plastic hinge rotation. This contributes to an increase in the lateral deflection ($w$) which in turn contributes to geometric deflection term ($\Delta_g$). The plastic hinge deforms axially until point C is reached. At the third region CDE of Fig. 1(b), the lateral deflection decreases considerably. This decrease is elastic and caused by a decrease in the $P$-$w$ moments induced by the decrease in the compressive load and by the change in sign of the $P$-$w$ moments with the application of a tensile load for portion DE. During this stage, the member continues to straighten while an increase tensile load is applied. Plastic hinge rotation is held constant during this region which in turns makes the third term ($\Delta_p$) of Eq. (1) constant.

At point E, the tension yielding starts due to the reversed bending moment due to lateral deflection and the tensile load. The plasticization in the center portion of the column results in a hardening behavior of the member as shown by the curve EF. Since the tensile $P$-$w$ moment reduces as the member straightens, the tensile load required to sustain yielding must increase. Thus, the stage EF has a monotonically increasing tensile load as the member lengthens. At point F, the member is fully straightened and the internal bending moments are essentially zero. Any further elongation beyond point F is purely plastic uniaxial elongation. The stage FG is characterized by a nearly constant tensile load $p$ with increasing elongation $\Delta$ for an elastic perfectly plastic material. If the tensile force is removed at this point, the member would remain essentially straight and be slightly longer than its original length. Point G is a load reversal point. Thus, the final stage GH consists of elastic unloading. The elongation will decrease linearly with decreasing tensile load, and the slope is essentially the same as that of the virgin elastic curve OA. Due to the plastic hinge formation in the hysteresis cycle, there is permanent deformation $\Delta_{OH}$ in the member as shown in Fig. 1(j).

### *2.3. Member axial load-axial deformation relations*

The approximate closed form relations between axial load versus axial deformation for a pin ended member Fig. 1(a) for various regions shown in Fig. 1(b) are presented in this section.

*(a) Elastic compression:* During the elastic compression (region OA) the axial deflection of a uniform member is given by Hooke's law and is equal to

$$\Delta = \Delta_e = \frac{PL}{AE} \tag{2}$$

in which, $L$, $A$, and $E$ represent length, area of cross section, and Modulus of elasticity respectively.

*(b) Elastic buckling:* The total axial deflection in stage AB, comprises of deflection ($\Delta_e$) due to elastic compression and deflection ($\Delta_g$) due to the change in geometry caused by lateral deflection ($w$). A small amount of axial load over the Euler buckling load causes the member to buckle in lateral direction. Fig. 2(a) shows free body diagram of member subjected to compressive load in the buckled configuration. Assume a sinusodial shape function for the bent shape:

$$w(x) = w_m \sin\frac{\pi x}{L} \tag{3}$$

where $w_m$ is the lateral deflection at the mid-section of the member. The axial deflection in elastic buckling phase is given by

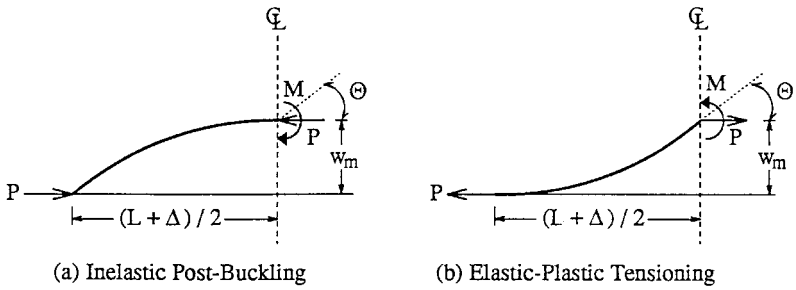


Fig. 2 Equilibrium forces in a buckling / tensioning member

$$\Delta = \Delta_e + \Delta_g = \frac{PL}{AE} - \frac{1}{2}\int_0^l \left(\frac{dw}{dx}\right)^2 dx \tag{4}$$

The second right hand term of Eq. (4) is the axial deflection due to lateral deflection (or buckling). After substituting Eq. (3) into Eq. (4), the total axial deflection is given by

$$\Delta = \frac{PL}{AE} - \frac{\pi^2 w_m^2}{4L} \tag{5}$$

$w_m$ is calculated using the equilibrium equation ($M = P\, w_m$) along with appropriate moment-axial load interaction curve. The interaction curve for ideal section, rectangular section and hollow circular section are taken as follows:

I-section:

$$\left|\frac{P}{P_y}\right| + \left|\frac{M}{M_p}\right| = 1 \tag{6}$$

Rectangular section:

$$\left|\left(\frac{P}{P_y}\right)^2\right| + \left|\frac{M}{M_p}\right| = 1 \tag{7}$$

Hollow circular-section:

$$c_1\left|\left(\frac{P}{P_y}\right)^2\right| + \left|\frac{M}{M_p}\right| = c_2 \qquad 0 \le \frac{P}{P_y} \le 0.65 \tag{8a}$$

$$c_3\left|\left(\frac{P}{P_y}\right)\right| + \left|\frac{M}{M_p}\right| = c_4 \qquad 0.65 \le \frac{P}{P_y} \le 1.0 \tag{8b}$$

where $P_y$ is the limit axial loading in pure tension and $M_p$ is the limit moment in pure bending. The empirical values for $c_1$, $c_2$, $c_3$, and $c_4$ in Eq. (8) for hollow circular cross section are taken as 1.50214, 1.273, 1.82, 1.82 respectively (Chen and Han 1985).

*(c) Inelastic post buckling:* The total axial deflection in the inelastic post buckling region, BC, consists of the deflection due to elastic compression ($\Delta_e$), deflection due to buckling ($\Delta_g$) and

deflection due to plastic hinge rotation at the mid section ($\Delta_p$). To find the $\Delta_g$ component, consider the moment curvature relation for a member subjected to compression (Fig. 2a)

$$\frac{d^2w}{dx^2} + \left(\frac{P}{EI}\right)w = 0 \tag{9}$$

where $E$, $I$, $w$ are the modulus of elasticity, moment of inertia and transverse displacement at a distance $x$ from the left support, respectively. The solution to Eq. (9) is given as

$$w = a_c \sin(kx) + b_c \cos(kx) \tag{10}$$

where $k = \sqrt{(P/EI)}$ and $a_c$, $b_c$ are constants to be determined from boundary conditions. Plastic hinge forms at point B (Fig. 1b), which is at the beginning of inelastic post-buckling. The boundary conditions for the member are $w(0)=0$ and $w(L/2)=w_m$. After substituting these boundary conditions into Eq. (10), the equation for lateral deflection is given as

$$w = w_m \frac{\sin\ kx}{\sin\left(\frac{kL}{2}\right)} \tag{11}$$

The axial deflection due to lateral deflection ($\Delta_g$) can be obtained after substituting Eq. (11) into the second term of Eq. (4) and is given as

$$\Delta_g = -L\left(\frac{kw_m}{2\sin\left(\frac{kL}{2}\right)}\right)^2\left[1 + \frac{\sin kL}{kL}\right] \tag{12}$$

The plastic deformation ($\Delta_p$) can be obtained from associated flow rule. The flow rule states that, when the state of stress is represented by a point on the yield curve, the plastic flow vector is in the direction of the outward normal to the yield curve at the corresponding stress point (Papadrakakis 1983). That is

$$\frac{d\Delta_p}{d\Theta} = -2\frac{dM}{dP} \tag{13}$$

where $\Theta$ is the slope at the mid length as shown in Fig. (2). The value of $dM/dP$ is obtained from the interaction curve of the cross section of the member. The interaction curve can be approximated by a number of linearized segments. Integrating Eq. (13) and substituting the boundary conditions $\Delta_p=0$ and $\Theta=0$ gives the expression for $\Delta_p$ at an axial load, $P$

$$\Delta_p = -2\left(\sum C_{i-1}\Delta\Theta_{i-1}\right) - 2C_i\Delta\Theta_n \tag{14}$$

The summation takes place through the history of plastic deformations. The index $i$ indicates the load increment and $n$ indicates last load increment. The terms $\Delta\Theta_{i\text{-}1}$ and $\Delta\Theta_n$ are the difference of the two slope angles corresponding to $P_{i\text{-}1}$, and $P_n$ respectively. $\Theta_i$ is slope of deflected shape at mid length of the member and can be obtained by differentiating the Eq. (11). The other

quantities are given as

$$C_i = \frac{M_{i+1} - M_i}{P_i - P_{i+1}}, \quad \Theta_i = \frac{k\, w_m}{\tan\left(\frac{kL}{2}\right)} \tag{15}$$

The total axial deflection during the inelastic post buckling region BC in Fig. 1(b) can be obtained from the following relation.

$$\Delta = \Delta_e + \Delta_g + \Delta_p \tag{16}$$

where $\Delta_e$, $\Delta_g$, $\Delta_p$ are given by Eq. (2), Eq. (12), and Eq. (14), respectively.

*(d) Elastic unloading and elastic tensioning:* The curve CDE consists of the axial deflection due to elastic compression, geometric deflection, and plastic deformation. Plastic deformation during this stage is constant (equal to $\Delta_p$ at point C) because of no plastic action in this region. The member is in compression during portion CD and changes sign to tension during portion DE.

Geometric deflection for portion CD. The constants $a_c$ and $b_c$ of Eq. (10) are to be determined from boundary conditions as $w(0)=0$ and $dw/dx(L/2)=\Theta$. After substituting these boundary conditions into Eq. (10), the equation for lateral deflection is given as

$$w = \frac{\Theta}{k\cos\left(\frac{kL}{2}\right)} \sin kx \tag{17}$$

The axial deflection due to lateral deflection ($\Delta_g$) can be obtained after substituting Eq. (17) into second term of Eq. (4) and is given as

$$\Delta_g = -L\left(\frac{\Theta}{2\cos\left(\frac{kL}{2}\right)}\right)^2 \left[1 + \frac{\sin kL}{kL}\right] \tag{18}$$

Geometric deflection for portion DE. Consider the moment curvature relation for a member subjected to tension (Fig. 2b)

$$\frac{d^2 w}{dx^2} - \frac{Pw}{EI} = 0 \tag{19}$$

The solution to Eq. (19) is given as

$$w = a_t \sinh kx + b_t \cosh kx \tag{20}$$

where $a_t$, $b_t$ are constants to be determined from boundary conditions. The constants ($a_t$ and $b_t$) are to be determined from boundary conditions as $w(0)=0$ and $dw/dx(L/2)=\Theta$. After substituting these boundary conditions into Eq. (20), the expression for lateral deflection is given as

$$w = \frac{\Theta}{k\cosh\left(\frac{kL}{2}\right)} \sinh kx \tag{21}$$

The total axial deflection in this region due to the lateral deflection ($\Delta_g$) can be obtained after substituting Eq. (21) into the second right hand term of Eq. (4) and is given as

$$\Delta_g = (-L)\left(\frac{\Theta}{2\cosh\left(\frac{kL}{2}\right)}\right)^2\left[1+\frac{\sinh kL}{kL}\right] \tag{22}$$

Thus, the total axial deflection during the elastic unloading and tensioning region, CDE, is given as:

$$\Delta = \Delta_e + \Delta_g + \Delta_p$$

$$\Delta_e = \frac{PL}{AE}$$

if $P \le 0$

$$\Delta_g = -\frac{L}{4}\left(\frac{\Theta}{\cos(kL/2)}\right)^2\left[1+\frac{\sin kL}{kL}\right]$$

if $P > 0$

$$\Delta_g = -\frac{L}{4}\left(\frac{\Theta}{\cosh(kL/2)}\right)^2\left[1+\frac{\sinh kL}{kL}\right] \tag{23}$$

*(e) Elastic-plastic tensioning:* The curve EF consists of axial deflection due to elastic compression, geometric deflection, and plastic deformation. Both geometric deformation and plastic deformation will reduce with increasing tension for equilibrium. At point F, a plastic hinge will form in tension. The geometric deflection and plastic deformation are computed in a manner similar to portion BC except the trigonometric functions are replaced by the hyperbolic functions. Therefore, the total axial deflection during this region is:

$$\Delta = \Delta_e + \Delta_g + \Delta_p$$

$$\Delta_e = \frac{PL}{AE}$$

$$\Delta_g = -L\left(\frac{kw_m}{2(\sinh(kL/2))}\right)^2\left[1+\frac{\sinh kL}{kL}\right]$$

$$\Delta_p = -2\left(\sum C_{i-1}\Delta\Theta_{i-1}\right) - 2C_i\Delta\Theta_n \tag{24}$$

*(f) Plastic tensioning and elastic unloading:* During the plastic tensioning stage (curve FG), the member behaves similar to perfectly elastic-plastic member, with a constant tensile force the deflection will increase. During the last stage of elastic unloading (curve GH), the member follows the original modulus of elasticity but with a permanent deformation in the member ($\Delta_{OH}$).

*(g) Compression/tension rupture:* During the hysteresis loop, after the member reaches point C, if the load in the member is neither reduced nor reversed sign to tension, then the member will fail by rupture due to the strain limitation in the members. Similarly, in the case of tension yielding, at point G, if the load is not reduced, then the member will fail by tension rupture.

### *2.4. Member failure in truss structures*

The change (decrease) in the member capacity during failure is represented by an additional ("pseudo") force vector applied externally at the member end joints. By introducing this load vector, the equations of motion of the damaged structure can be written in terms of mass, damping and stiffness matrices of the intact structure. This scheme has been used for linear analysis by Malla *et al.* (1995), Malla and Nalluri (1995). This scheme is now extended for nonlinear dynamic analysis in this study. The pertinent equations of motion for the structure in intact and damaged states can be written as:

*For intact structure*

$$[M]\{\ddot{y}\} + [C]\{\dot{y}\} + ([K_e] + [K_g])\{y\} = \{P_s\} + \{P_d\} \tag{25}$$

where $\{\ddot{y}\}$, $\{\dot{y}\}$, and $\{y\}$ are acceleration, velocity and displacement vectors, respectively, of the intact structure. $[M]$, $[C]$, $[K_e]$ and $[K_g]$ represent mass, damping and elastic and geometric stiffness matrices of the intact structure. $\{P_s\}$ and $\{P_d\}$ are externally applied static and dynamic load vectors, respectively.

*For damaged structure*

$$[M']\{\ddot{y}'\} + [C']\{\dot{y}'\} + ([K'_e] + [K'_g])\{y'\} = \{P_s\} + \{P_d\} \tag{26}$$

where $\{\ddot{y}'\}$, $\{\dot{y}'\}$, and $\{y'\}$ are acceleration, velocity and displacement vectors, respectively, of the damaged structure. $[M']$, $[C']$, $[K'_e]$ and $[K'_g]$ represent mass, damping and elastic and geometric stiffness matrices of the damaged structure.

The equation of motion for the damaged structure if expressed in terms of intact structural properties, Eq. (26) can be written as:

$$[M]\{\ddot{y}'\} + [C]\{\dot{y}'\} + ([K_e] + [K_g])\{y'\} = \{P_s\} + \{P_d\} - \{F_n\} \tag{27}$$

The additional load vector, $\{F_n\}$ arising from the member failure is given as:

$$\{F_n\} = ([M'] - [M])\{\ddot{y}'\} + ([C'] - [C])\{\dot{y}'\} + \{([K'_e] - [K_e]) + ([K'_g] - [K_g])\}\{y\} \tag{28}$$

### *2.5. Solution methodology*

The solution to the nonlinear equation of motion (Eq. 27) can be obtained by using numerical step-by-step integration schemes. The response history is divided into a sequence of short time steps, and during each time step the response is calculated. Step-by-step integration scheme assumes that the solution for the discrete time $t$ is known, and the solution for the discrete time ($t$+$\Delta t$) is required, where $\Delta_t$ is suitably chosen time increment. It is assumed that the mass and stiffness of the structure remains constant during a time step. Newmark method is chosen for the present study and this method approximates the relations between displacements, velocities and accelerations as follows:

$$\{y\}^{t+1} \approx \{y\}^t + \{\dot{y}\}^t \Delta t + \left(\frac{1}{2} - \alpha\right)\Delta t^2 \{\ddot{y}\}^t + \Delta t^2 \alpha \{\ddot{y}\}^{t+1} \tag{29}$$

$$\{\dot{y}\}^{t+1} \approx \{\dot{y}\}^t + \Delta t(1-\beta)\{\ddot{y}\}^t + \Delta t \beta \{\ddot{y}\}^{t+1} \tag{30}$$

where the superscripts $t$ indicates the quantities at the present time step and $t$+1 indicates the quantities at the next time step. The parameters $\alpha$ and $\beta$ represents the variation of the acceleration. In the present study, $\alpha$=0.25 and $\beta$=0.5 are chosen to represent the constant average acceleration method which is unconditionally stable for numerical integration.

The equation of motion of the damaged structure can be written after substituting Eq. (29) and Eq. (30) into Eq. (27) as follows:

$$[K_{eff}]\{y'\}^{t+1} = \{F'(y', \dot{y}', \ddot{y}')\}^{t+1} \tag{31}$$

where

$$[K_{eff}] = \left[\left(\frac{1}{\alpha\Delta t^2}\right)[M] + \left(\frac{\beta}{\alpha\Delta t}\right)[C] + [K_e] + [K_g]\right] \tag{32}$$

$$\begin{aligned}\{F'(y', \dot{y}', \ddot{y}')\}^{t+1} &= \{P_s\} + \{P_d\}^{t+1} - \{f'\}^{t+1} + \\ &[M]\left[\left(\frac{1}{\alpha\Delta t^2}\right)\{y'\}^t + \left(\frac{1}{\alpha\Delta t}\right)\{y'\}^t + \left(\frac{1}{2\alpha} - 1\right)\{y'\}^t\right] + \\ &[C]\left[\left(\frac{\beta}{\alpha\Delta t}\right)\{y'\}^t + \left(\frac{\beta}{\alpha} - 1\right)\{y'\}^t + \left(\frac{\beta}{2\alpha} - 1\right)\Delta t\{y'\}^t\right]\end{aligned} \tag{33}$$

in which

$$\begin{aligned}\{f'\}^{t+1} &= \left(\frac{1}{\alpha\Delta t^2}\right)([M'] - [M])\{y'\}^{t+1} + \left(\frac{\beta}{\alpha\Delta t}\right)([C'] - [C])\{y'\}^{t+1} + \\ &([K'_e] - [K_e])\{y'\}^{t+1} + ([K'_g] - [K_g])\{y'\}^{t+1}\end{aligned} \tag{34}$$

The structural response of the intact structure can be obtained by substituting $\{f'\}^{t+1}$=0 and $\{y\}$, $\{\dot{y}\}$ and $\{\ddot{y}\}$ for $\{y'\}$, $\{\dot{y}'\}$ and $\{\ddot{y}'\}$ respectively in the Eq. (31) to Eq. (34).

The pseudo force $\{f'\}$ represents the member capacity deviation from the linear elastic response of the intact structure. Pseudo force vector is modified at every time step and applied at the end joints of the member. The modified Newton Raphson iterative method is used for solving nonlinear equations of motion Eq. (31). The updating of the nodal point displacements in the iteration is continued until the out-of-balance loads and incremental displacements are small. A computational code DYNFAIL based on a nonlinear finite element analysis technique is developed to solve the nonlinear equations of motion (Nalluri 1996).

## 3. Application and results

Fig. 3 shows a two-dimensional nine-bay aluminum truss which is simply supported at the ends (hinge at node 1 and roller support at node 18). The structural geometric parameters and material properties are given in Table 1. Fig. 4 shows the axial load versus axial deformation behaviour of diagonal and chord members of the truss structure as given by the expressions presented under section entitled “Axial load-axial deformation relations.” Since the present example dealt with the compression region only, these curves were not generated for full cycle. Except member 15 (due to reason given below), all other members are considered to follow these paths. Table 1 also lists Euler

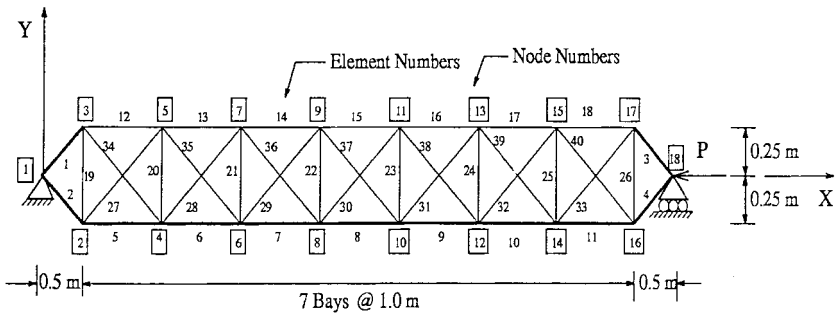


Fig. 3 Two-dimensional nine bay planar truss structure

Table 1 Nine bay planar truss - Material and geometry

Material: Aluminum (2014-T6); Modulus of Elasticity, $E$=70.0 GPa; Density, $\rho$=2710 Kg/m$^3$; Yield Stress, $\sigma_Y$=95.0 MPa.
Geometry: All members are circular tubes (outer diameter=30 mm)

| Element No. | Thickness (mm) | Slenderness Ratio | Euler Critical Stress (MPa) | $\Delta_A$ (mm) | $\Delta_B$ (mm) |
|---|---|---|---|---|---|
| 1 - 4 | 3.7 | 59.53 | 194.943 | 1.556758 | 2.169237 |
| 5 - 11 | 3.7 | 106.49 | 60.916 | 0.870227 | 0.994475 |
| 12 - 18 | 3.0 | 104.11 | 63.733 | 0.910471 | 1.017582 |
| 19 - 26 | 3.0 | 52.06 | 254.932 | 1.820932 | 3.520943 |
| 27 - 40 | 3.0 | 116.40 | 50.989 | 0.814374 | 1.076834 |

$\Delta_A$=Axial displacement at the start of Elastic buckling (Point A in Fig. 4b);
$\Delta_B$=Axial displacement at the start of Inelastic postbuckling (Point B in Fig. 4b)

critical stress for each member and axial displacements at the critical elastic and postbuclkling points. A parabolic axial load and moment interaction relation was used. Members 1 to 4 and 19 to 26 may fail by compression yielding before buckling and hence, the member capacity curves are not presented here.

Lumped mass finite element model of the structures was considered for the analysis. The geo-

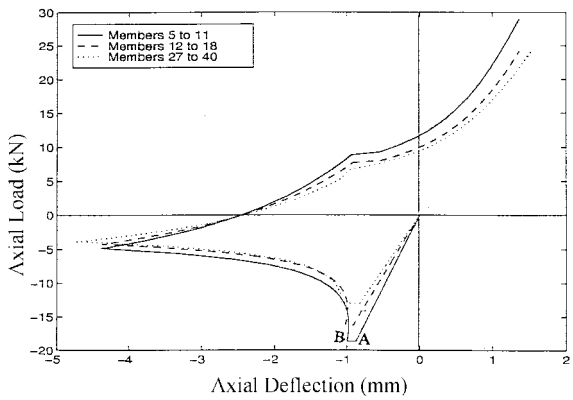


Fig. 4 Actual member behavior curves

metrical stiffness, $[K_g]$, of a member was not considered for this example. Only undamped response were obtained. The natural frequencies of the intact structure corresponding to modes 1, 2, 3, 4 and 63 (last degree of freedom) were 127.58 (period=0.04925 s), 478.92, 782.51, 979.43 and 13153.55 radians per second, respectively.

The structure is loaded with a static load of magnitude of 45.0 kN at node 18 in the negative $X$-axis direction. The load is applied in a ramp fashion (Fig. 5) with a rise time of 0.2 s which is more than 4 times the first natural period of the intact structure, thus is essentially equivalent to a statically applied load.

When the external load of magnitude 45.0 kN is fully applied, the stresses in all the members are well below the Euler buckling stress for a compression members and yield stress for the tension members. Member 15 is considered to fail first within the elastic regime point B (Fig. 6a), where the member has axial force of $F_0$ (=14.4665 kN) and axial displacement of $\Delta_1$ (=0.812142857 mm). Member 15 is chosen to lose load carrying capacity in four different fashions as shown in Fig. 6(a): Case (i) is the intact structure where all members are intact and behave in the elastic regime. In Case (ii), member 15 loses all its load carrying capacity at point $C_b$ when its axial deflection is 3 times $\Delta_1$. In Case (iii), member 15 loses all its load carrying capacity at point $C_c$ when its axial deflection is 2.25 times $\Delta_1$. In Case (iv), the capacity of member 15 is zero when its axial deflection equals to 1.01 times $\Delta_1$ at point $C_d$. Case (iv) thus represent a sudden member failure scenario. The structural response (joint deflections and member axial forces) were obtained for a total duration of

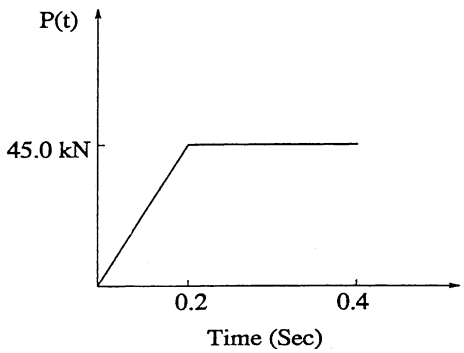


Fig. 5 Externally applied load details

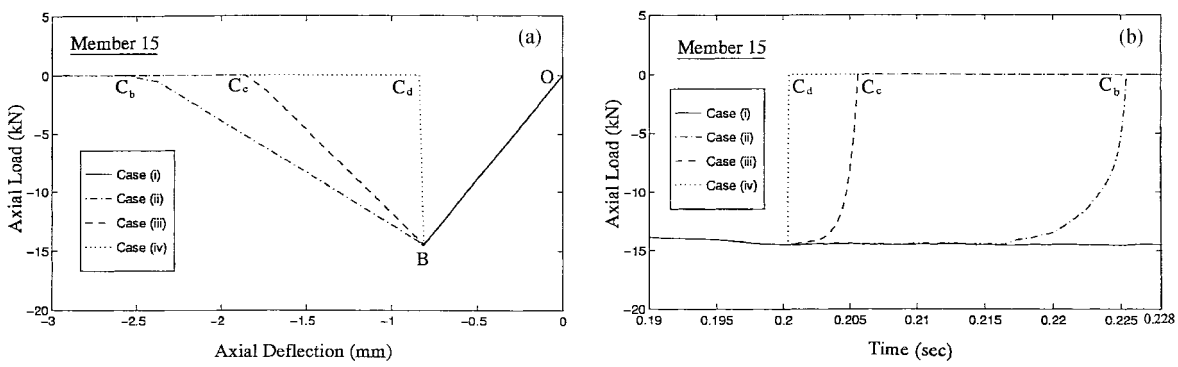


Fig. 6 Member 15 response: (a) axial force-axial deformation relation; (b) time variation of member force

0.3 s with a time step size of 0.00008 s. Only some sample results are presented below due to space limitation in the manuscript.

Fig. 6(b) shows the time variations of axial force in member 15 for all 4 cases. Member 15 took 0.02552 s, 0.00560 s, and 0.0004 s to travel from point B where the member has full load carrying capacity to reach, respectively, points $C_b$, $C_c$, and $C_d$ where it has zero load capacity. The time variation of displacement of Node 18 is shown in Fig. 7. The time variations of axial forces in members 7 and 8 are shown in Figs. 8 and 9, respectively. Members 7, 14, 22, 29 and 38 were in the elastic region only. But it was observed that the axial load in the members changed from tension to compression or compression to tension. Member 8, 11, 30, 37 have gone through inelastic postbuckling during the failure propagation. Table 2 shows the sequence of member failure (and/or entry into postbuckling regime).

## 4. Conclusions

An analytical and computational procedure has been developed to study the response of truss

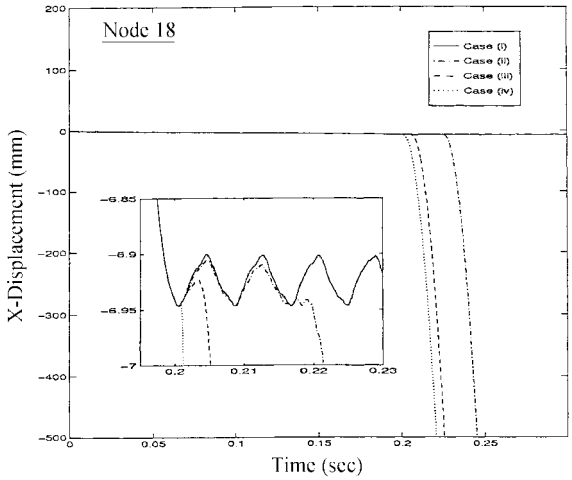


Fig. 7 Time variation of Node 18 displacement

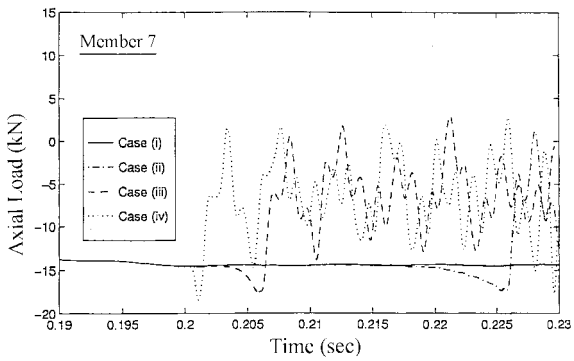


Fig. 8 Variation of force in Member 7 with time

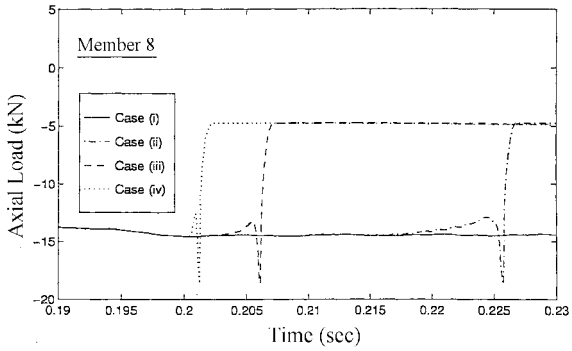


Fig. 9 Variation of force in Member 8 with time

Table 2 Structural failure sequence

| Time (s) | Member Number | | |
|---|---|---|---|
| | Brittle | E. B. | I. P. B. |
| CASE (i) | All members intact and elastic | | |
| CASE (ii) | | | |
| 0.20040 | 15 | | |
| 0.22432 | | 30, 37 | |
| 0.22528 | | | 30, 37 |
| 0.22568 | | 8 | |
| 0.22584 | | | 8 |
| CASE (iii) | | | |
| 0.20040 | 15 | | |
| 0.20528 | | 30, 37 | |
| 0.20576 | | | 30, 37 |
| 0.20608 | | 8 | |
| 0.20616 | | | 8 |
| CASE (iv) | | | |
| 0.20040 | 15 | | |
| 0.20072 | | 30, 37 | |
| 0.20088 | | | 30, 37 |
| 0.20120 | | 8 | |
| 0.20128 | | | 8 |
| 0.21280 | | | 11 |

E. B. = Elastic Buckling;
I. P. B. = Inelastic Postbuckling

structures undergoing member failure under applied static and dynamic loadings. Emphasis has been given to the dynamic effects of member failure and the propagation of local damage in the structure. The material nonlinearity is modeled in member axial load versus axial deflection space. Geometric nonlinearity is included while computing the stiffness of the structure. The present methodology allows any type of member axial load and axial deflection relations to be adopted

easily. The method includes actual member loading and unloading behavior in elastic, elastic buckling, inelastic postbuckling, and tension yielding regions; and the rate of member capacity reduction, thus modeling the possible sudden member snap in the postbuckling regime. The pseudo-force vector is used to represent the member capacity reduction. The structural response obtained using the nonlinear finite element analysis technique can be presented in terms of joint displacements, stresses, and member forces as a function of time. The methodology developed was applied to a planar nine-bay indeterminate truss structure. The results showed that failure of one single member may cause propagation of failure of several members in the structure.

## Acknowledgements

The authors acknowledge the partial financial support obtained from the National Science Foundation, U.S.A. under Grant MSS-9110900 and the University of Connecticut. The results reported in this paper in part were presented at the Third Asian-Pacific Conference on Computational Mechanics held in Seoul, Korea during Septemeber 16-18, 1996 (Malla and Nalluri 1996).

## References

ASCE Task Committee on Latticed Structures under Extreme Loads (1984), "Dynamic consideration in latticed structures", *J. of Struct. Engnrng.*, **110**(10), *ASCE*, New York, 2547-2551.

Bathe, K.-J. (1982), *Finite Element Procedures in Engineering Analysis*, Prentice- Hall, N.J.

Blandford, G. and Wang, S. (1993), "Response of space trusses during progressive failure", *Dynamic Response and Progressive Failure of Special Structures* (R. Malla, Ed.), *ASCE*, New York, 1-16.

Chen, W.F. and Han, D. (1985), *Tubular Members in Offshore Structures*, Pitman Publishers, Inc., MA, U.S.A.

Davies, G. and Neal, B.G. (1959), "The dynamical behavior of a strut in a truss framework", *Proc. Royal Society.*, **A253**, 542-562.

Malla, R.B. and Nalluri, B. (1994), "Response of truss structures subjected to dynamic loads during member failure", *Spatial, Lattice and Tension Structures* (J. Abel, J. Leonard, and C. Penalba, Eds.), *ASCE*, New York, 249-258.

Malla, R.B. and Nalluri, B. (1995), "Dynamic effects of member failure on the response of truss type space structures", *J. of Spacecraft and Rockets*, **32**(3), *AIAA*, 545-551.

Malla, R.B. and Nalluri, B. (1996), "A computational technique to model member failure in truss structures", *Proceedings of the Third Asian-Pacific Conference on Computational Mechanics* (Eds: C.-K. Choi, C.-B. Yun and D.-G. Lee), Seoul, Korea, **1**, Sept., 415-421.

Malla, R.B., Wang, B. and Nalluri, B. (1993), "Dynamic effects of progressive member failure on the response of truss structures", *Dynamic Response and Progressive Failure of Special Structures* (R. Malla, Ed.), *ASCE*, NY, Dec., 60-76.

Malla, R.B., Wang, B. and Nalluri, B. (1995), "Dynamic member failure in trusses by Pseudo-force method", *Int. J. of Space Struct.*, **10**(2), Multi-Science Publish. Co., U.K. 99-112.

Morris, N. (1993a), "Effect of member snap on space truss collapse", *J. of Engineering Mechanics*, **119**(4), *ASCE*, New York, 870-886.

Morris, N. (1993b), "Effect of member snap on progressive collapse of space structures", *Dynamic Response and Progressive Failure of Special Structures* (R. Malla, Ed.), *ASCE*, New York, 17-31.

Murtha-Smith, E.A. (1988), "Alternate path analysis of space trusses for progressive collapse", *J. of Struct. Engnrg.*, **114**(9), 1978-1999.

Nalluri, B.B. (1996), "Non-linear dynamic effects of member failure in truss structures", Ph.D. Dissertation,

Dept. of Civil & Env. Engnrg., Univ. of Connecticut, Storrs, U.S.A.

Nonaka, T. (1973), "An elastic-plastic analysis of a bar under repeated axial loading", *Int. J. Solids Structures*, **9**(5), 569-580 (Erratum: **9**(10)).

Nonaka, T. (1977), "Approximation of yield condition for the hysteric behavior of a bar under repeated axial loading", *Int. J. Solids Structures*, **13**, 637- 643.

Papadrakakis, M. (1985), "Inelastic cyclic analysis of imperfect columns", *J. of Struct. Engnrg., ASCE*, **111**(6), 1219-1234.

Schmidt, L.C., Morgan, P.R. and Clarkson, J.A. (1976), "Space trusses with brittle type strut buckling", *J. of the Struct. Div., ASCE*, **102**(ST7), 1479-1492.